JOURNAL OF VIROLOGY, Dec. 2008, p. 12291–12303 Vol. 82, No. 24
0022-538X/08/$08.00+0 doi:10.1128/JVI.01383-08

Epigenetic Silencing of Human Immunodeficiency Virus (HIV) Transcription by Formation of Restrictive Chromatin Structures at the Viral Long Terminal Repeat Drives the Progressive Entry of HIV into Latency▽

Richard Pearson, Young Kyeung Kim, Joseph Hokello, Kara Lassen, Julia Friedman, Mudit Tyagi, and Jonathan Karn*

Department of Molecular Biology and Microbiology, Case Western Reserve University School of Medicine, Cleveland, Ohio

Received 2 July 2008/Accepted 22 September 2008

The molecular mechanisms utilized by human immunodeficiency virus (HIV) to enter latency are poorly understood. Following the infection of Jurkat T cells with lentiviral vectors that express Tat in *cis*, gene expression is progressively silenced. Silencing is greatly enhanced when the lentiviral vectors carry an attenuated Tat gene with the H13L mutation. Individual clones of lentivirus-infected cells showed a wide range of shutdown rates, with the majority showing a 50% silencing frequency between 30 to 80 days. The silenced clones characteristically contained a small fraction (0 to 15%) of activated cells that continued to express d2EGFP. When d2EGFP$^+$ and d2EGFP$^-$ cell populations were isolated from the shutdown clones, they quickly reverted to the original distribution of inactive and active cells, suggesting that the d2EGFP$^+$ cells arise from stochastic fluctuations in gene expression. The detailed analysis of transcription initiation and elongation using chromatin immunoprecipitation (ChIP) assays confirms that Tat levels are restricted in the latently infected cells but gradually rise during proviral reactivation. ChIP assays using clones of latently infected cells demonstrate that the latent proviruses carry high levels of deacetylated histones and trimethylated histones. In contrast, the cellular genes IκBα and GAPDH had high levels of acetylated histones and no trimethylated histones. The levels of trimethylated histone H3 and HP1-α associated with HIV proviruses fell rapidly after tumor necrosis factor alpha activation. The progressive shutdown of HIV transcription following infection suggests that epigenetic mechanisms targeting chromatin structures selectively restrict HIV transcription initiation. This decreases Tat production below the levels that are required to sustain HIV gene expression.

The vast majority of human immunodeficiency virus (HIV) infections result in active viral transcription and replication; however, in a few rare cases the virus can enter a long-lived latent state in which viral gene expression is silenced. Although the pool of latently infected cells is very small (approximately 1 in 10^6 resting CD4$^+$ T cells in the peripheral circulation), the ability to latently infect cells helps HIV to establish chronic infections despite strong humoral and cellular immune responses and to evade intensive antiretroviral therapy. Siliciano and his colleagues (29, 41) have proposed that the generation of latently infected cells is a consequence of normal maturation and cellular differentiation events leading to the formation of quiescent T-cell populations. For example, if an activated effector T cell becomes infected by HIV when it is in the process of reverting to being a resting memory T cell, a stably integrated but transcriptionally silent form of the provirus can be generated. Similarly, Zack and colleagues have effectively used the HIV SCID-hu (Thy/Liv) mouse model to recapitulate the generation of latent HIV during thymopoiesis (1, 4, 5). As infected CD4$^+$ CD8$^+$ thymocytes differentiate and mature, there is a shutdown of HIV transcription and the entry of the cell into a quiescent state. Thus, for both naïve and memory T cells, latency can occur following the infection of an activated precursor cell that subsequently shuts down.

The entry of HIV into latency is regulated at the molecular level by the expression of the viral *trans*-activator protein Tat (for reviews, see references 2 and 23). Tat is unique because it acts primarily, if not exclusively, at the level of elongation. In the absence of Tat, the majority of RNA polymerase II (RNAP II) complexes that have initiated transcription dissociate from the template near to the promoter (22). Tat stabilizes the elongating RNA polymerase and permits the efficient synthesis of full-length HIV transcripts. Tat is recruited to the HIV promoter by binding to TAR, a stem-loop RNA encoded by the first 59 nucleotides of the viral mRNAs. The binding of Tat to TAR requires cooperative interaction with human CycT1, a component of the transcriptional elongation factor P-TEFb (46). The recruitment of P-TEFb (a complex of hCycT1 and CDK9) through its interactions with Tat and TAR results in the activation of the CDK9 kinase and the consequent phosphorylation of a variety of proteins within the elongating transcription complex, including the C-terminal domain of RNAP II, forming a highly phosphorylated form of the polymerase called RNAP II_o* (25). The modification of the transcription complex to make it more processive also requires the phosphorylation of specific cofactors, including Spt5, a subunit of the DRB sensitivity-inducing factor that enhances transcriptional elongation (3, 20), and the E subunit of the elongation

* Corresponding author. Mailing address: Department of Molecular Biology and Microbiology, Case Western Reserve University, 10900 Euclid Avenue, Room W200, Cleveland, OH 44106-4960. Phone: (216) 368-3915. Fax: (216) 368-3055. E-mail: jonathan.karn@case.edu.
▽ Published ahead of print on 1 October 2008.

repressive factor NELF (13). Thus, the net effect of recruiting P-TEFb through its interactions with Tat and TAR is to remove blocks to transcription elongation through the phosphorylation of Spt5 and NELF-E and to simultaneously stimulate polymerase processivity through the phosphorylation of the large subunit of RNA polymerase.

The design of this regulatory circuit means that conditions that restrict transcription initiation will, in turn, cause a reduction in Tat levels to below threshold levels and therefore result in dramatically reduced HIV transcription. Weinberger et al. (47–49) have argued persuasively that stochastic fluctuations in Tat gene expression provides one of the earliest regulatory decisions in this circuit. However, most investigators agree that in latently infected cells, a variety of additional restrictions serve to limit initiation and prevent new Tat synthesis. These blocks include the presence of inhibitory chromatin structures (18, 21), the absence of positive factors that are required for initiation (i.e., NF-κB or NF-AT) (27, 39), and decreased levels of P-TEFb (15, 16, 19, 43). Although many factors have been associated with the development of latency, the sequence of events and the contribution of individual factors to the repression of the long terminal repeat (LTR) are largely unknown.

In this paper, we have utilized lentiviral vectors that express Tat in *cis* to monitor the entry of HIV into latency. We have found that although viruses expressing wild-type Tat can give rise to latently infected cells, a much higher proportion of proviruses are shut down when cells are infected with viruses expressing an attenuated Tat gene. Studies of individual clones have demonstrated that transcription from the lentiviral LTR progressively declines in virtually all clonal populations, but both the rate and degree of shutdown is highly variable between individual clones. Once silenced, transcription from latent HIV proviruses can be efficiently reactivated by the induction of NF-κB. Remarkably, the viruses quickly reenter latency once NF-κB is withdrawn. The analysis of the latently infected clones by chromatin immunoprecipitation (ChIP) assays suggests that epigenetic restrictions involving specific chromatin modifications are responsible for the shutdown of transcription observed during the entry of the infected cells into latency.

MATERIALS AND METHODS

Plasmid constructs. pHR′-p-d2EGFP was derived by inserting the EcoRI-XhoI fragment of HIV-1_{pNL4-3} into the pHR′ plasmid (10). A short linker containing the Kozak sequence and an MluI site were inserted between the stop codon of *env* and the XhoI site in *nef*. d2EGFP (Clontech) was inserted between the MluI and XhoI sites. Site-directed mutagenesis was performed to construct the Tat variants. Cysteine 22 was mutated to glycine (TGT to GGA), and histidine 13 was changed to leucine (CAT to TTA) as described previously (42). Site-directed mutagenesis was used to introduce the mutant NF-κB (mNF-κB) binding sites within the LTR region (50).

Infection of Jurkat T cells by lentiviral vectors. Vesicular stomatitis virus G-pseudotyped HIVs were produced by the triple transfection of 293T cells using Lipofectamine as described previously (26). The vector titer was determined by the infection of 1×10^6 Jurkat T cells with a serial dilution of the harvested medium supernatant. Mixed populations of infected Jurkat T cells were maintained in RPMI 1640 medium supplemented with 10% fetal bovine serum (FBS), penicillin (100 IU/ml), streptomycin (100 μg/ml), and 25 mM HEPES at 37°C in 5% CO_2. Eight hours postinfection, cells were washed and the RPMI medium was replaced. d2EGFP expression levels were assessed using flow cytometry 48 h postinfection. The mixed populations were sorted by flow cytometry to develop 100% d2EGFP-positive mixed populations and, subsequently, clonal cell lines. Changes in d2EGFP expression levels within the mixed populations were recorded on a weekly basis via fluorescence-activated cell sorting (FACS) for up to 40 days.

Cloned cell lines. Clones were isolated by sorting single cells into individual wells of 96-well microtiter plates. Clones were cultivated and assessed for d2EGFP expression 3 weeks after the sort date. The shutdown of d2EGFP-positive clones was recorded on a weekly basis via FACS for up to 175 days. Clones also were isolated from lentiviral vector-infected populations of Jurkat C63 cells (Tat^+).

Reactivation and shutdown of clones. Clones were activated by treatment with 10 ng/ml tumor necrosis factor alpha (TNF-α) for 2, 4, 6, 8, and 16 h, and samples were analyzed for d2EGFP expression via FACS. Cells that had been treated for 16 h were washed twice with RPMI 1640, resuspended in RPMI 1640 medium supplemented with 10% FBS, penicillin (100 IU/ml), streptomycin (100 μg/ml), and 25 mM HEPES, and incubated at 37°C in 5% CO_2. The cells were analyzed by FACS at 24-h intervals starting after the washing step for a total of 6 days. Shutdown analysis was performed by measuring both the percentage of d2EGFP-positive cells and the mean fluorescence intensity (MFI) of the population. Detailed shutdown kinetics for clone 2D10 (H13L Tat) cells were obtained by monitoring changes in d2EGFP expression every 2 h after TNF-α removal for up to 48 h. In a parallel experiment, the cells were treated with 0.25 μg/ml of cycloheximide (CHX) following the removal of TNF-α.

Wild-type Tat (clone E4), H13L Tat (clone 2D10), C22G Tat (clone 2B2D), and mNF-κB LTR/H13L Tat (clone 2B5) were activated by treatment with 10 ng/ml TNF-α for 16 h and imaged using a Deltavision-RT epifluorescence microscope (Applied Precision Inc., Issaquah, WA). The cells were stained with 4′,6′-diamidino-2-phenylindole (DAPI) and actin antibodies (Molecular Probes) prior to imaging.

ChIP analysis of the kinetics of RNAP II recruitment following cell stimulation. Jurkat T-cell populations were activated using 10 ng/ml of TNF-α. For each time point, 5×10^7 cells were fixed with formaldehyde (0.5%) and prepared for ChIP as previously described (26). Immunoprecipitations were performed using the N-20 antibody (Santa Cruz) against the RNAP II large subunit. DNA was eluted from the protein A-Sepharose beads using 300 μl of sodium dodecyl sulfate lysis buffer containing 2 μl proteinase K (10 mg/ml) at 50°C for 2 h. Five times binding buffer (buffer PB; Qiagen) was added to each sample, and the DNA was isolated by using QiaQuick columns (Qiagen). SYBR green PCR master mix (12.5 μl; Bio-Rad) combined with 1 μl of each primer and 8.5 μl of ChIP sample was analyzed by real-time PCR. Primers used were the following: HIV nucleosome 1 region (forward, +30-CTG GGA GCT CTC TGG CTA ACT A; reverse, +134-TTA CCA GAG TCA CAC AAC AGA CG, where "+30" indicates the nucleotide after the transcription start site); HIV envelope region (forward, +2599-TGA GGG ACA ATT GGA GAA GTG A; reverse, +2697-TCT GCA CCA CTC TTC TCT TTG C); GAPDH promoter (forward, −125-CAC GTA GCT CAG GCC TCA AGA C; reverse, −10-AGG CTG CGG GCT CAA TTT ATA G); and IκBα 5′ end (forward, +155-AAG AAG GAG CGG CTA CTG GAC; reverse, +237-TCC TTG ACC ATC TGC TCG TAC T).

Analysis of HIV chromatin structure. ChIP experiments were performed on clone 2D10 cells as described previously (26) using the following antibodies: anti-RNAP II-N20 (SC-899); anti-histone H3, CT, pan, and clone A3S (05-928; Upstate); anti-acetyl-histone H3 (Lys9/18) (07-593; Upstate); anti-trimethyl-histone H3 (Lys9) (07-442; Upstate); anti-trimethyl-histone H3 (Lys27) (07-449; Upstate); and HP1α-C15 (SC-10210).

Real-time PCR was performed using the HIV nucleosome 1 region and the IκBα 5′-end primers described above, as well as a slightly modified set of GAPDH promoter primers (forward, −145-TAC TAG CGG TTT TAC GGG CG; reverse, +21-TCG AAC AGG AGG AGC AGA GAG CGA).

Integration site analysis. Genomic DNA (gDNA) was isolated from $\sim 5 \times 10^6$ cells for each clone examined, and 2 μg of gDNA was digested with NdeI (2 μl) or EcoRI (2 μl) (NEB). Digested gDNA (240 ng) was ligated overnight to create circularized DNA fragments (17). Nested PCR then was performed using primers specific to the HIV genome. Products isolated from the PCRs were sequenced to determine the flanking sequences of gDNA and were analyzed using the BLAT alignment tool (http://genome.ucsc.edu/) (24).

RESULTS

Progressive silencing of HIV. Most molecular studies of HIV latency have relied on the selection of rare, latently infected clones from large populations of infected cell lines (6, 21, 28). Because only a few rare infections gave rise to latently infected cells, a limitation of these studies was that it was not

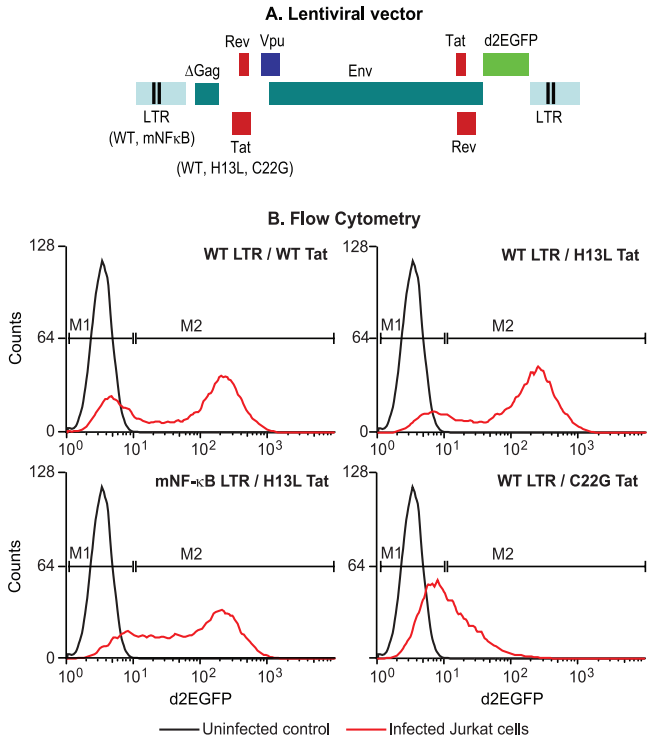

FIG. 1. Lentiviral vectors expressing Tat and Rev in *cis*. (A) Genomic organization of the lentiviral vectors. A fragment of HIV-1_{pNL4-3}, containing *tat*, *rev*, *env*, and *vpu*, was cloned into the pHR′ backbone (10). The reporter gene d2EGFP was inserted into this construct in the position of the HIV *nef* gene. Three additional variants of this wild-type (WT) vector were developed by inserting mutations into either the LTR (mNF-κB) or the Tat gene (H13L and C22G). (B) Flow cytometry of newly infected cells. Following the production of single-round, infectious particles using the lentiviral triple transfection system, equal titers of each virus were used to infect 1×10^6 Jurkat T cells. Forty-eight hours following infection, the cells were assessed for d2EGFP expression by FACS. WT, wild type.

possible to monitor the events associated with entry into latency. In the experiments described here, we have exploited lentiviral vectors expressing attenuated Tat variants to generate a much higher frequency of latently infected cells and to permit the study of epigenetic events leading to HIV silencing.

An important feature of the vectors we have developed is that, like HIV itself, they are activated in *cis* by the regulatory proteins Tat and Rev and therefore are able to sustain the positive feedback circuit that regulates HIV transcription (Fig. 1A) (26). The viruses carried either the wild-type Tat gene or the H13L mutation, a partially attenuated Tat variant originally identified in the U1 latently infected cell line (12). In order to evaluate Tat-independent transcription, vectors have been created in which Tat is inactivated by the C22G mutation in the Zn^{2+} binding domain (14).

To facilitate the monitoring of infection frequencies and HIV transcription, we have followed the strategy of Jordan et al. (21) and introduced fluorescent reporter proteins in place of the *nef* gene. In order to provide a more effective measurement of transcription rates we have utilized the d2EGFP protein, which has a reduced half-life of 3.6 h (see Fig. 5B) due to the addition of the PEST sequence from mouse ornithine decarboxylase at the C terminus (8).

Populations of Jurkat T cells were infected with each type of virus and assessed for d2EGFP expression by FACS (Fig. 1B). Although the H13L mutation was previously reported to be a poor activator of HIV transcription in transient transfection assays (12, 42), Jurkat T cells infected with vectors containing either the wild-type or the H13L Tat gene were able to express d2EGFP to similar levels. By contrast, the C22G mutation, which prevents Tat association with P-TEFb (14, 42), reduced d2EGFP expression approximately 10-fold, demonstrating the strong dependency of HIV transcription on a functional Tat protein.

To assess the role of NF-κB, we also evaluated viruses carrying mutations of GGG to CTC in both NF-κB-binding sites to prevent NF-κB binding to the HIV enhancer (50). Surprisingly, the inactivation of the NF-κB-binding sites did not noticeably restrict the levels of d2EGFP expression, demonstrating that NF-κB is not essential for transcription when the provirus is first integrated into the host genome (Fig. 1). However, as described below, NF-κB is essential for the activation of HIV transcription in latently infected cells. These observations are consistent with reports indicating that NF-κB is largely dispensable for virus growth in most transformed cell lines (7, 32).

Experiments performed with viruses packaged with defective integrase confirm that the initial expression levels observed in these experiments were due to integrated proviruses rather than the carryover of vector DNA or expression from unintegrated viral DNA (data not shown).

Although there is a high level of HIV transcription immediately after infection, the frequency of cells expressing high levels of d2EGFP fell progressively as the infected cell populations were grown over the next few weeks. A trivial explanation for the loss of HIV expression is that uninfected cells gradually outgrow the infected cell population. For example, there could be a selective growth advantage for the uninfected cells due to the expression of potentially toxic products produced by the provirus, such as Tat or Env or even d2EGFP itself.

To rule out this possibility and to monitor the shutdown phenomenon in more detail, freshly infected Jurkat T cells were sorted into $d2EGFP^+$ populations. As shown in Fig. 2, both the rate of shutdown and the proportion of cells losing d2EGFP expression was dramatically increased for cells infected with viruses carrying H13L Tat instead of wild-type Tat. After 35 days of culture, more than 50% of the cells carrying the H13L proviruses had shut down, whereas less than 20% of cells carrying the wild-type Tat had shut down. In numerous experiments we have noted that the majority of cells infected with the H13L viruses will eventually shut down, whereas 20% seems to be an upper limit for the number of cells carrying wild-type viruses that will become latent within the timeframe of these experiments. As described in detail below, virtually all of the cells in the $d2EGFP^-$ population can be reactivated following the induction of NF-κB, demonstrating that the proviruses in these cells have been silenced but remain transcriptionally competent.

Expression of Tat in *trans* blocks entry of viruses into latency. To test the hypothesis that entry into latency is associ-

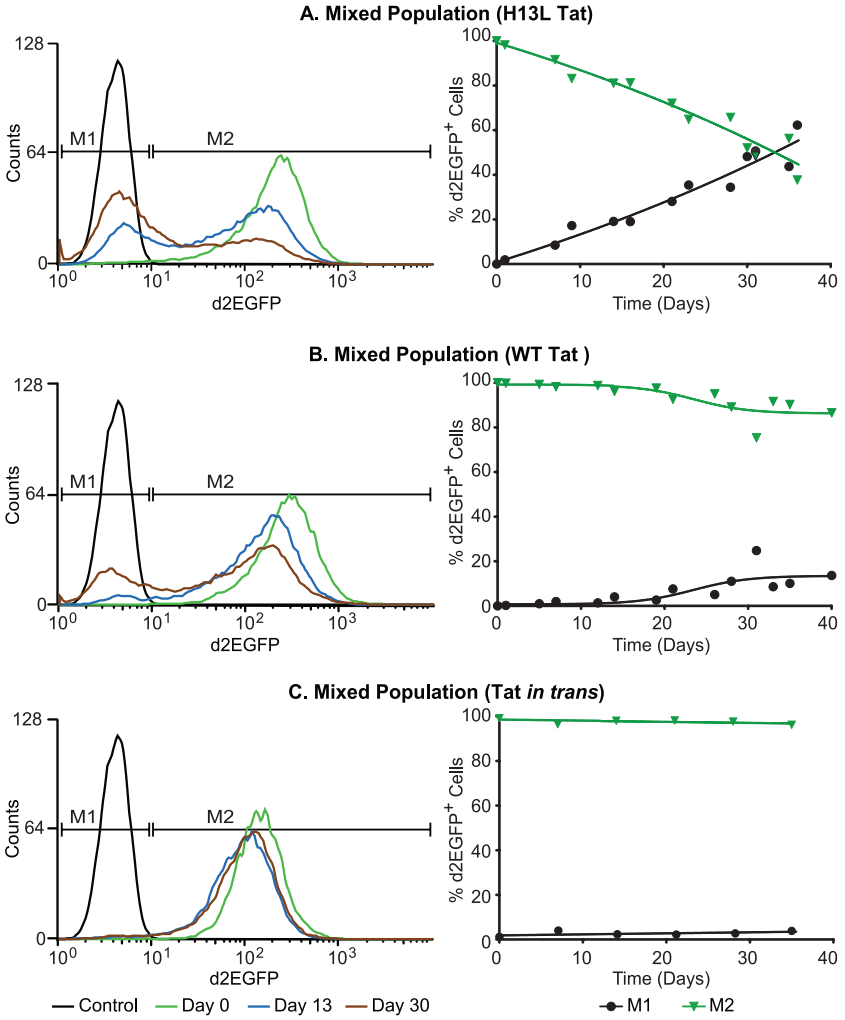

FIG. 2. Progressive silencing of lentivirus-infected Jurkat T cells. Freshly infected, mixed populations of Jurkat T cells were sorted by FACS to obtain populations of 100% d2EGFP$^+$ cells. d2EGFP expression for each cell population was measured by FACS during a 40-day period. (A) Silencing of cells infected with the H13L Tat vector. (B) Silencing of cells infected with the wild-type Tat vector. (C) Constant transcription of the H13L Tat vector in Jurkat C63 cells, which constitutively express Tat from a retroviral vector. The left panels show representative FACS profiles of the cell populations at various times during the experiment (i.e., uninfected Jurkat T cells [black lines]; 0 days [green lines]; 13 days [blue lines]; and 30 days [brown lines]). In order to quantitatively measure the number of cells that were infected and expressing d2EGFP, gates were set as shown on the profiles. The panels on the right show plots of the percentage of d2EGFP$^+$ cells. The M1 region corresponds to cells that are no longer expressing d2EGFP (black lines), while the M2 region contains cells showing detectable levels of d2EGFP expression (green lines). Because of the extremely high reproducibility of the silencing rates, data for the plots were combined from three separate experiments and fitted to sigmoidal curves.

ated with breaking the Tat-dependent regulatory circuit, we examined the rate of transcriptional silencing in cells that constitutively express Tat. Jurkat C63 cells were prepared by infecting Jurkat T cells with murine retroviruses that express Tat under the control of the LTR. After the infection of Jurkat C63 cells with the H13L viruses, d2EGFP expression remained high in mixed cell populations throughout extensive time courses (Fig. 2C) as well as in clonal cell lines (data not shown).

NF-κB and Tat are required for reactivation of latent proviruses. Figure 3 presents examples of clonal cell lines that were isolated from the d2EGFP-negative portion of a partially shut down, mixed population of infected Jurkat T cells. The Jurkat E4 clone carries wild-type Tat, whereas the 2D10 clone was isolated from cells infected with the H13L virus. Both clones show an extremely high degree of transcriptional restriction before the induction of NF-κB by TNF-α. Prior to activation, more than 95% of the infected E4 or 2D10 cells show no detectable reporter gene expression. Maximal levels of d2EGFP can be induced in over 80% of the E4 cells and more than 98% of the 2D10 cells after the treatment of the cells for 18 to 24 h with TNF-α. An advantage of these clones over the J-Lat 6.3 model for HIV latency, which has been extensively used by Greene and colleagues (21, 51, 52), is that although J-Lat 6.3 cells also are latently infected, only 30% of the J-Lat 6.3 cells can be reactivated under these conditions. The extensive reactivation of the E4 and 2D10 clones demonstrates that few, if any, of the cells have lost the latent provi-

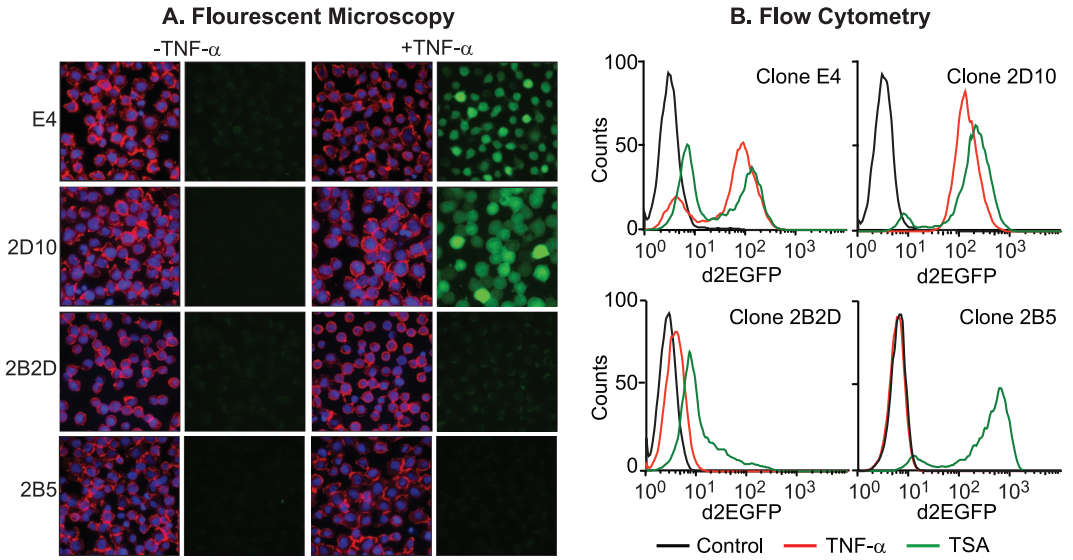

FIG. 3. Activation of latently infected Jurkat T-cell clones by TNF-α or TSA. Cells were induced for 16 h with 10 ng/ml TNF-α or with 500 nM TSA. Clonal cell lines were isolated for vectors carrying wild-type Tat and the wild-type LTR (E4), H13L Tat and the wild-type LTR (2D10), C22G Tat and the wild-type LTR (2B2D), and H13L Tat and the mNF-κB LTR (2B5). (A) Microscope images of TNF-α-activated clones. In the left panels, DAPI (blue) and actin (red) stains were utilized in the fluorescence microscopy to identify the number of cells in the field of view. The right panels show d2EGFP expression from the same field (green). (B) Flow cytometry of clones activated by TNF-α or TSA. Black lines, cells before induction; red lines, cells induced by TNF-α; green lines, cells induced by TSA.

ruses. These clones also were efficiently activated by treatment with the histone deacetylase inhibitor trichostatin A (TSA), suggesting that chromatin restrictions are partially responsible for the maintenance of the latent phenotype.

In contrast, latently infected cells carrying proviruses with C22G Tat could not be efficiently reactivated by TNF-α. Although there is a small shift in the d2EGFP levels, the overall level of transcription following TNF-α treatment is severely restricted by the absence of Tat. Treatment with TSA resulted in the activation of the entire cell population, although only a small minority of the cells showed transcription levels as high as those seen in the Tat-positive clones. Similarly, clones isolated from cells infected with the virus bearing the mutant NF-κB binding sites (clone 2B5) are unresponsive to TNF-α. However, these cells can be efficiently activated by TSA (Fig. 3B), suggesting that a primary function of NF-κB is to help remove chromosomal restrictions on initiation in the latently infected cells.

Epigenetic silencing of HIV proviruses in clonal cell populations. The progressive shutdown process we observed using the H13L Tat mutation strongly suggests that epigenetic silencing events are responsible for the generation of latently infected clones. To confirm this hypothesis, we decided to monitor the silencing of cells derived from individual d2EGFP$^+$ cells. Figure 4A and B shows the behavior of eight representative clones from two experiments. Forty-eight hours after infection with the H13L virus, individual cells that expressed high levels of d2EGFP were sorted into wells. The clones were expanded for 3 weeks before assessment for the initial d2EGFP levels was possible and then were monitored for d2EGFP expression using FACS for the next 176 (Fig. 4A) or 77 days (Fig. 4B).

The clones showed a wide range of shutdown rates, and each achieved a stable end state with a unique proportion of cells that carried silenced proviruses. A few clones, such as clone D7 (Fig. 4A) and clone 1 (Fig. 4B), showed rapid shutdown kinetics and were greater than 90% d2EGFP negative by 4 weeks. In contrast, a small number of clones showed delayed shutdown kinetics, with clone G5 (Fig. 4A) being an extreme example that took approximately 150 days to reach 50% silencing. However, the majority of the clones showed a 50% silencing frequency of 30 to 80 days (e.g., clones G6 and D4 [Fig. 4A] and clones 5, 6, and 8 [Fig. 4B]). Although there is a large degree of clonal variation, these experiments demonstrate that the epigenetic shutdown of proviral transcription is observed in the majority of clones isolated from the mixed population and that latency is not limited to a few rare proviruses that fortuitously integrate into restrictive regions of the genome.

The proviral integration sites for each of the clones described in this paper have been sequenced and located within the host genome (Table 1). The majority of our clones are single integrants, although a few double integrants also were detected. As expected from the extensive studies characterizing HIV proviral integration sites (33, 34, 38), the majority of clones were located in intronic regions of host genes. We also have confirmed that clones 2D10 and E4 carry the H13L and wild-type Tat genes, respectively, and there have been no mutations in the LTR in either clone.

Kinetics of proviral reactivation by NF-κB and reversion to latency is uniform between different clones. To determine whether clones that had been silenced show similar reactivation profiles, we analyzed the reactivation kinetics of four clones that showed wide variation in their initial rates of shutdown (Fig. 4C). The rate of reactivation for each of the clones was essentially identical, with 50% of the cells becoming d2EGFP$^+$ in 3.54 ± 0.85 h.

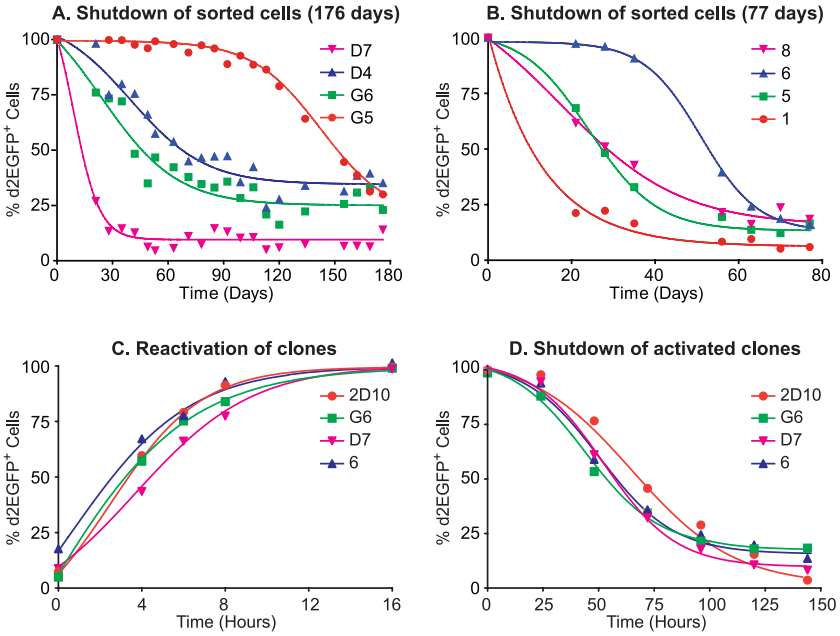

FIG. 4. Individual latently infected cells show unique silencing rates but similar reactivation kinetics. (A) Jurkat T cells were infected with the H13L Tat vector, and d2EGFP-positive clones were isolated by the sorting of individual cells into the wells of 96-well microtiter plates. The graphs show the percentage of d2EGFP$^+$ cells (M2 region) with the data fitted to sigmoidal curves to obtain accurate values for the silencing rates. Due to the time required to obtain enough cells for flow cytometry, the initial time point is 21 days following the initial sorting. Eight representative clones were monitored at weekly intervals for up to 176 days. (B) An experiment similar to that shown in panel A, but shutdown was monitored for 77 days. (C) Reactivation of clones D7, G6, 2D10, and 6. Cells were treated with TNF-α (10 ng/ml) and monitored for d2EGFP expression at 4, 6, 8, and 16 h poststimulation. (D) Shutdown of activated clones. Following the 16-h reactivation period with TNF-α, the cells were washed twice in RPMI and then assessed for d2EGFP expression at 24-h intervals for a total of 6 days. Sigmoidal curves (variable slope) were fitted to all data sets.

To monitor the return to latency, TNF-α was removed after 16 h and the proportion of d2EGFP-positive cells was monitored at 24-h intervals (Fig. 4D). The return to the basal state was much more rapid than the original shutdown, with all the clones examined reverting to their respective off states within just 6 days. This uniformity in shutdown rates is striking compared to that of the original shutdown data. We noted that each clone reverts to its characteristic starting condition with a fixed proportion of activated cells present in the population as described below.

In Fig. 4D, we measured the fraction of cells that express d2EGFP. Additional information about the kinetics of proviral reactivation and shutdown can be obtained by measuring the mean fluorescence intensity for each population (Fig. 5B). Clone 2D10 cells were activated by TNF-α, washed, and analyzed at 2-h intervals over the next 48 h (Fig. 5A). In a parallel experiment, the activated cells were treated with CHX to assess the half-life of the d2EGFP protein and to measure the maximal rate at which the system can be shut down when no new protein synthesis is permitted (Fig. 5A). The CHX-treated cells shut down in a very uniform manner and displayed a half-life of 3.6 h for d2EGFP. In contrast, in the untreated population the removal of TNF-α results in two phases of d2EGFP decline and much slower kinetics than those seen following CHX treatment (Fig. 5B). There is an initial lag from 0 to 4 h, followed by a rapid decline in d2EGFP expression over the next 8 h (half-life of 5.9 h). During this period, there is a uniform shift in the cell populations to lower expression levels (Fig. 5A). After 12 h, the decay in mean fluorescence intensity slows considerably and begins to decline, with a half-life of 25.5 h. In contrast to the first phase, the distribution of activated and inactivated cells is very heterogeneous (Fig. 5A).

Our interpretation of the complex kinetics is that the initial phase corresponds to the rapid decline in transcription initiation due to the loss of NF-κB from the system when TNF-α is removed. During the second, slower phase, there is a high degree of cell-to-cell variation in expression levels. This behavior is consistent with a slow decline in Tat levels and the associated stochastic behavior of the Tat feedback mechanism (47).

Stochastic fluctuations in HIV transcription determine the extent of clonal silencing. The analysis of the FACS data used to generate Fig. 4 also demonstrates that individual cells within each clonal population display a wide range of d2EGFP expression levels. This indicates that even when the integration sites are identical, there is still significant epigenetic variation between each individual cell. In addition, although most of the clones we evaluated eventually reached a point where 50% or more of the cells became latently infected, only a few clones achieved latency in more than 90% of the cells. For each clone there appears to be a unique point at which the population was stable and there were no further declines in the percentage of d2EGFP-expressing cells.

To determine whether the d2EGFP-positive cells represent a population of constitutively active cells, the clones G6 and 6

TABLE 1. Proviral integration sites

Cell type	Clone identity	LTR	Tat	No. of integrants	Integration site	Gene name or description	Intron or exon	Orientation with respect to cellular promoter
Jurkat	2D10	WT	H13L	1	Chr16: 1,931,379-1,931,920	Selenoprotein X, 1	Exon	←
Jurkat	E4	WT	WT	1	Chr9: 94,160,412-94,160,777	Hypothetical protein LOC401541	Intron	→
Jurkat	2B2D	WT	C22G	1	Chr9: 133,268,876-133,269,180	KIAA0515 (uc004cam.1)	Intron	←
Jurkat	2B5	mNF-κB	H13L	1	Chr6: 33,384,022-33,384,454	Human gene TAPBP	Intron	←
Jurkat	1	WT	H13L	1	Chr22: 23,093,648-23,093,997	Cytospin-A	Intron	→
Jurkat	8	WT	H13L	1	Chr3: 198,330,000-198,330,120	DLG1	Intron	→
Jurkat	G6	WT	H13L	1	Chr12: 52,153,359-52,153,733	Poly(rC)-binding protein 2 isoform	Intron	←
Jurkat	G5	WT	H13L	1	Chr6: 143,241,294-143,241,611	HIVEP2	Intron	→
Jurkat	D7	WT	H13L	1	Chr12: 109,456,620-109,505,447	T-cell activation protein phosphatase 2C	Intron	→
Jurkat	5	WT	H13L	2	Chr14: 106,063,269-106,063,392 and Chr4: 187,236,961-187,237,129	Uncharacterized region of the genome and Toll-like receptor 3	Unknown and exon	Unknown and ←
Jurkat	6	WT	H13L	2	Chr8: 126,084,856-126,085,757 and Chr8: 136,699,760-136,700,530	Squalene mono-oxygenase and KH domain-containing RNA-binding signal	Intron and intron	← and ←
Jurkat	D4	WT	H13L	2	Chr17: 71,564,456-71,564,893 and Chr15: 87,625,552-87,625,680	Gene SRP68 and gene KIAA1794	Exon and intron	← and →
Jurkat C63	9	WT	WT in *trans*	1	Chr1: 98,042,043-98,042,208	Dihydropyrimidine dehydrogenase	Intron	←

→, Provirus integrated in same the orientation as the gene promoter. ←, Provirus integrated in opposite orientation of gene promoter.

were sorted into d2EGFP$^+$ and d2EGFP$^-$ populations and monitored via FACS analysis (Fig. 6). These clones were chosen because they had distinct subpopulations of activated cells representing 9 and 16% of the population, respectively. Consistent with the observations of Weinberger et al. (47), the clonal populations are not static and the spontaneous reactivation and shutdown of individual cells is continuously occurring. Within 24 h, the d2EGFP$^-$ cells reestablished a transcriptionally active d2EGFP$^+$ subpopulation at essentially the same level as that of the original clonal population. Similarly, the d2EGFP$^+$ population shut down, although the time required to establish the same ratio of d2EGFP$^+$- to d2EGFP$^-$-expressing cells as the unsorted population takes more than 8 days. Thus, each clone is able to establish a unique and stable equilibrium state with a nearly constant proportion of transcriptionally active cells. The continuous reversions between a transcriptionally active and inactive state strongly suggests that stochastic fluctuations in the balance between positive factors, such as the levels of NF-κB and other transcription initiation factors in the system, and negative factors, such as the extent of histone deacetylation, determine whether any given cell will become transcriptionally active.

NF-κB and Tat are strictly required for proviral reactivation. The reactivation of HIV transcription from a transcriptionally silent provirus requires the restoration of the Tat-dependent feedback circuit. To assess our clones for changes in transcription initiation and elongation following TNF-α stimulation, we treated clones 6 (H13L Tat), 2B2D (C22G tat), 2B5 (mNF-κB), and Jurkat C63 clone 9 (Tat in *trans*) with TNF-α and performed ChIP experiments using an antibody to RNAP II to monitor the distribution of transcription complexes along the proviral DNA. As seen in Fig. 7A, the recruitment of RNAP II to the nucleosome region of the provirus, which is near the start site of transcription and therefore provides a measurement of transcription initiation, is cyclical and corresponds to the fluctuating levels of NF-κB p65 in the nucleus (26, 53).

In the experiment using clone 6 (H13L Tat), approximately 2.5 cycles of NF-κB activation were detected over a 4-h time course (Fig. 7, top). To illustrate the cyclic nature of RNAP II recruitment to the promoter, the data were fitted to a series of Gaussian distributions. The curve fitting allowed the accurate measurements of the underlying periodicities in the data and demonstrated the remarkably consistent induction kinetics.

To provide a measurement of transcription elongation, RNAP II levels were monitored in the vector's HIV *env* gene, approximately 2,600 nucleotides downstream of the transcription start site (Fig. 7B). The underlying periodicity in RNAP II levels also is evident in these data, but we noted that the maximum level of RNAP II grew with each successive wave. The levels of RNAP II at the distal regions reached or exceeded the promoter levels during the third wave at around 240 min. This is consistent with the idea that the initial restricted rounds of transcription elongation proceed in the absence of Tat. As Tat levels rise due to the new synthesis of the protein, it is able to stimulate RNAP II elongation following successive waves of HIV transcription initiation. Very similar kinetic results were obtained using clones 2D10 (H13L Tat) and E4 (wild-type Tat) (data not shown).

In these experiments, the cellular genes IκBα and GAPDH were utilized as internal controls. The IκBα gene is NF-κB responsive and acts as a positive control for NF-κB levels in the nucleus. As shown in Fig. 7C, the IκBα gene has three peaks of RNAP II recruitment following TNF-α activation that have the

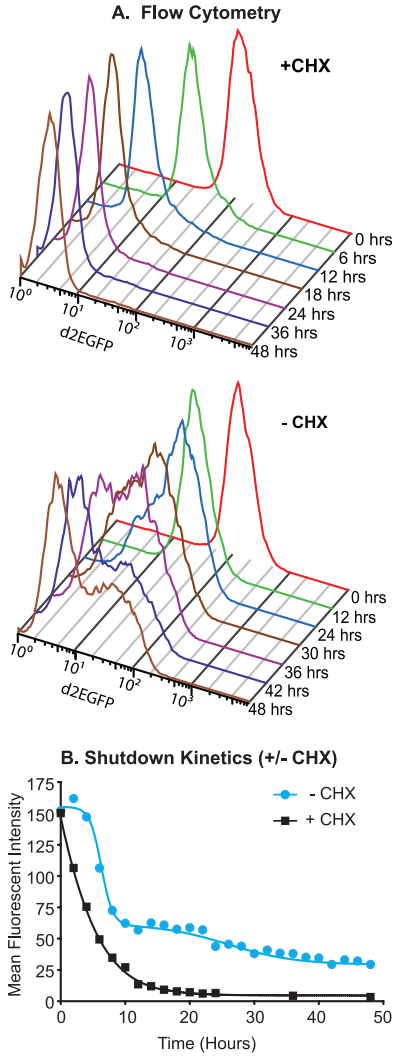

FIG. 5. Detailed analysis of the shutdown of clone 2D10 following TNF-α reactivation. (A) Representative FACS profiles of cell populations during shutdown in the presence (+) and in the absence (−) of 0.25 μg/ml CHX. (B) Graph of the mean fluorescence intensity demonstrating progressive reductions in d2EGFP levels during the shutdown. A one-phase decay curve was fitted to the CHX-treated samples (black line), and a biphasic curve was fitted to the untreated samples (blue line).

same periodicity as that seen at the HIV LTR. However, the levels of RNAP II at this control gene dampen after the second peak, suggesting that although both promoters respond to NF-κB mobilization, each promoter is regulated distinctly.

The GAPDH gene is both constitutively active and NF-κB independent. Whereas both the IκBα and HIV promoters have low levels of RNAP II prior to TNF-α stimulation, the level of RNAP II at the GAPDH promoter already is comparable to the maximal levels of RNAP II seen on the NF-κB-responsive genes. During the 4-h time course, there is a general increase in GAPDH transcription but there is no evidence for reproducible underlying fluctuations in gene expression (Fig. 7D). Since we were unable to reproducibly fit curves to this data, the data were simply fitted with a straight line for the purposes of illustration.

Additional ChIP experiments using clones carrying mutations in the NF-κB sites and Tat were performed to confirm the distinct roles of these transcription factors in regulating initiation and elongation during proviral reactivation (Fig. 7). Clone 2B2D contains a provirus carrying the C22G Tat mutation. As expected, although there is efficient recruitment of RNAP II to the promoter-proximal region following increases in initiation caused by TNF-α, very little RNAP II is found in the downstream region of the provirus. Unexpectedly, the pattern of RNAP II recruitment to the promoter showed a reproducible, subtle kinetic difference, with the second peak of RNAP II associated with the promoter delayed by approximately 20 min (to 170 ± 15 min) compared to that of clones with functional Tat genes, such as clone 6 (142 ± 8 min). This suggests that Tat plays an indirect role in regulating initiation by enhancing promoter clearance or helping to remove chromosomal restrictions near the promoter. The examination of clone 2B5 (Fig. 7) demonstrates that the mutations at the NF-κB DNA-binding domains prevent both the initiation and recruitment of RNAP II to the promoter.

Jurkat C63 clone 9 (Fig. 7) illustrates the impact constitutive Tat expression in *trans* has on the transcription behavior of an integrated provirus. In this clone there is more than twice the amount of RNAP II associated with the provirus. A second important difference is that the rapid increases in RNAP II levels at the promoter following stimulation are closely matched by the changes in the levels of RNAP II downstream. This is because there is no restriction on elongation due to the absence of sufficient levels of Tat, as in the case of the latently infected clones. The IκBα and GAPDH cellular control genes in this clone give responses very similar to those seen in the other clones examined and suggest that the constitutive expression of Tat has no effect on their expression profiles.

Latent proviruses accumulate heterochromatic markers at the viral LTR. In order to correlate changes in chromatin structure with events taking place during proviral reactivation, we used ChIP experiments to compare the levels of several key chromatin markers and RNAP II at the promoter of clone 2D10 and the two control gene promoters, IκBα and GAPDH (Fig. 8). In this experiment we also compared the unstimulated clone to those at the 30- and 150-min time points following activation by TNF-α, which correspond to the first and second peaks of RNAP II seen in the time course studies shown in Fig. 7. As expected, levels of RNAP II at both the provirus and the IκBα gene are low initially and then increase three- to fourfold in response to NF-κB activation. In contrast, the levels at the GAPDH promoter are stable and high. The total amount of histone H3 (Fig. 8B) at the promoter region was at constant levels for the LTR and both of the control genes and was unaffected by stimulation. However, as shown in Fig. 8C, the HIV LTR was markedly depleted in acetylated histone H3 at the LTR compared to the IκBα or GAPDH promoter. Both promoters showed increases in acetylated histones following TNF-α activation, but much greater increases were observed at the IκBα gene. In fact, the IκBα promoter has much greater levels of acetylation even prior to stimulation than that observed at the LTR. The levels of histone H3 acetylation seen at the GAPDH promoter also were much greater than those seen at the LTR and remained constant after TNF-α stimulation.

Recent reports by du Chéné et al. (9), Marban et al. (36),

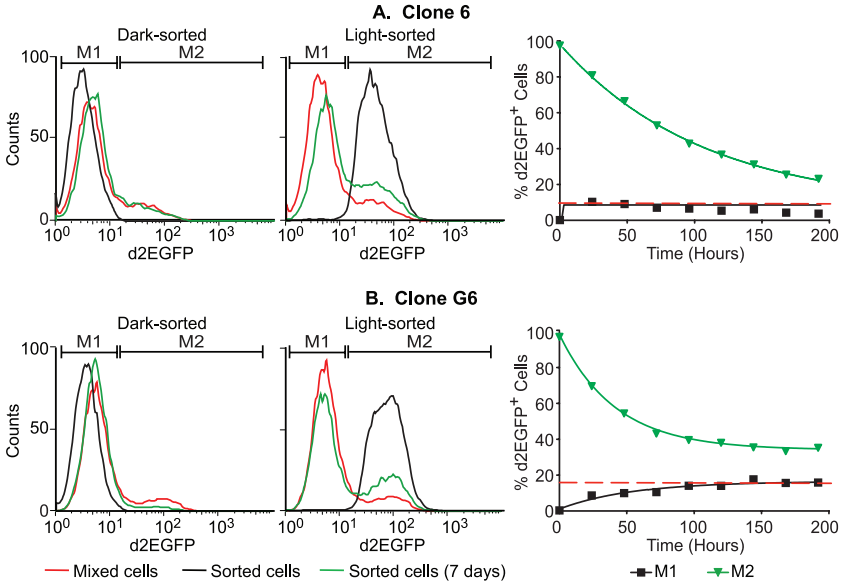

FIG. 6. Spontaneous reactivation and shutdown of latently infected clones. Two latently infected clones that showed measurable levels of spontaneously activated cells were sorted into populations of d2EGFP$^+$ and d2EGFP$^-$ cells (clone 6 and clone G6 in Fig. 4). FACS analysis of the cell populations immediately following cell sorting are shown by the black lines. The same cell populations were analyzed after 8 days (green lines). For comparison, the unsorted population is shown by the red lines. Each sorted population was monitored for any changes in the levels of d2EGFP expression at 24-h intervals for 8 days. The scatter plots represent the observed number of cells in each population (green triangle, d2EGFP$^+$ sort; black squares, d2EGFP$^-$ sort) that expressed d2EGFP during the time course with one-phase decay curves fitted. The dotted red line indicates the average percentage of d2EGFP$^+$ cells seen in the unsorted clonal population over the same time period. (A) Clone 6; (B) clone G6.

and Mateescu et al. (37) have implicated factors involved in histone methylation as mediators of HIV latency. We therefore examined the levels of trimethylated histone H3 modified at lysine 27 or 9 and the levels of the methylated histone binding protein HP1-α. As shown in Fig. 8D to F, trimethylated histones were observed at the LTR prior to activation, but these repressive markers were absent from the two control genes. The levels of trimethylated histone H3 Lys 27, Lys 9, and HP1-α fell rapidly after TNF-α activation.

These data clearly indicate the contrasting impact of the epigenetic restrictions placed on the integrated provirus and the unrestricted IκBα gene, despite the fact that they both respond similarly to the transcription factor NF-κB. The hypoacetylation at the LTR, combined with the presence of trimethylated histones prior to stimulation, imply that the LTR is actively repressed, whereas the IκBα gene is simply inactive in the absence of NF-κB.

DISCUSSION

Epigenetic silencing of HIV transcription is a primary event mediating entry into latency. As first reported by Cloyd and his colleagues (35, 44), a long-standing, but puzzling, observation is that chronically infected cell lines gradually accumulate latently infected cells. Weinberger et al. (47) also observed a gradual shift toward latency in cells infected with replication-deficient HIV-1 vector. However, a limitation of all these experiments is that it was not possible to determine whether the enrichment of latently infected cells was due to selective pressures on the populations, leading to an enrichment of already transcriptionally inactive subsets of cells, or whether the viruses genuinely entered latency.

In this paper, we have been able to directly demonstrate the shut down of HIV transcription leading to latency by monitoring HIV silencing in isolated clones infected with lentiviral vectors expressing Tat in *cis*. The shutdown profiles in Fig. 4 show that the time required for silencing in the majority of clones is surprisingly long, with times typically ranging from 30 to 80 days to achieve 50% shutdown.

It is important that despite the fact that all of the cells within these clonal populations are derived from the same progenitor cell and therefore share a common proviral integration site, there is considerable variation in transcription between individual cells. At every stage in the experiment we are able to detect a subset of cells in the population that have become transcriptionally silent, while other cells are still expressing high levels of d2EGFP. This simple observation strongly implies that entry into latency is not hard wired into the viral LTR, nor is it simply a function of the viral integration site; rather, the epigenetic control mechanisms play an important role in mediating the shutdown of viral transcription.

Jordan et al. (21) developed the popular J-Lat series of latently infected cell lines by isolating clones from the rare population of cells that were immediately transcriptionally silenced. Here, we have followed a different strategy and isolated latent clones from populations of cells that were initially transcriptionally active (i.e., d2EGFP$^+$). The isolation of clones from the low/no transcription pool using the protocol of Jordan et al. (21) appears to significantly enrich for cells in which the provirus has fortuitously integrated in either alphoid

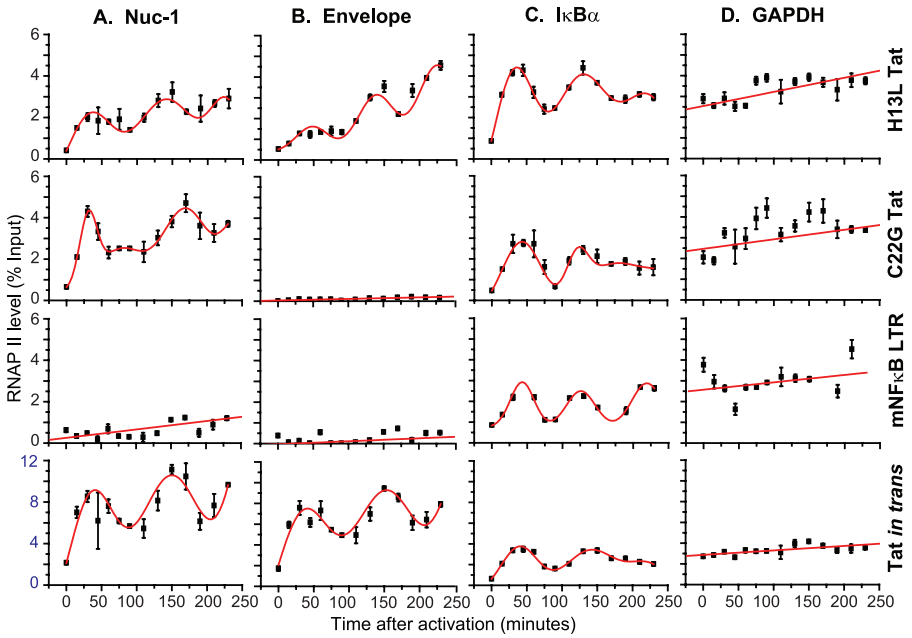

FIG. 7. Proviral reactivation requires both NF-κB and Tat expression. RNAP II levels at the HIV LTR (A), HIV *env* region (B), and the promoters of two control genes, IκBα (C) and GAPDH (D), were measured by ChIP assays using the N-20 antibody. Analyses were performed on clone 6 (wild-type LTR and H13L Tat), 2B2D (wild-type LTR and C22G Tat), 2B5 (mNF-κB LTR and H13L Tat), and Jurkat C63 clone 9 (wild-type LTR and H13L Tat plus wild-type Tat expressed constitutively). Cells were activated by 10 ng/ml TNF-α, and samples were taken every 15 min for the first 90 min, followed by sampling at 20-min intervals until the completion of the time course. Individual data sets were normalized to the average GAPDH level and fitted to a series of Gaussian distributions for the HIV and IκBα genes. The GAPDH data were fitted to a straight line, since the data showed no reproducible underlying periodicity.

repeats, gene deserts, or highly transcribed genes (33). Recently, Lenasi et al. (31) demonstrated that many of the clones are subject to transcriptional interference caused by the elongating RNAP II transcribing through the viral promoter. In contrast, we have found by direct sequence analyses that all of the proviruses in our latently infected clones are integrated in random orientations into euchromatic regions of the genome within transcription units expected to be active in Jurkat T cells. Although our sample size is comparatively small, our observations are consistent with the results of recent high-throughput sequencing studies of HIV integration sites from both resting $CD4^+$ T cells isolated from HIV-infected patients and infected T-cell lines that have shown that the vast majority of proviruses are integrated within active host genes and are rarely found in heterochromatic regions (17, 33).

Evidence that epigenetic silencing is responsible for HIV

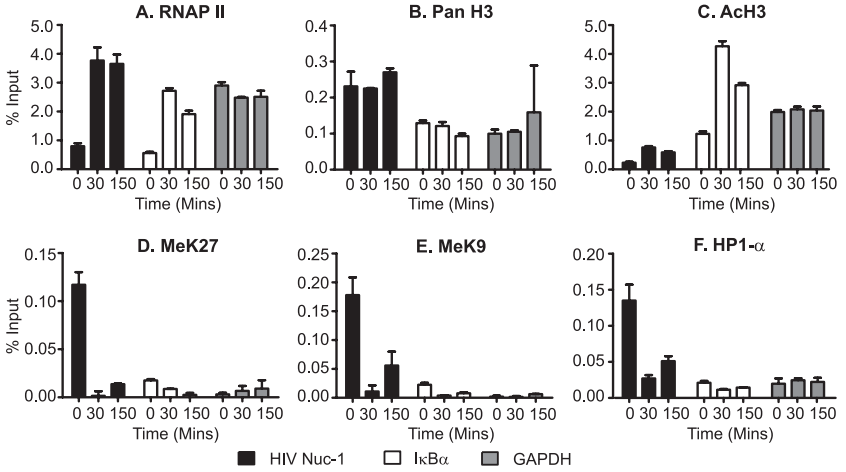

FIG. 8. Latent proviruses carry trimethylated histones. 2D10 cells were stimulated with 4 ng/ml of TNF-α, and samples were isolated after 30 or 150 min and compared to an unstimulated control (0 min). Samples were analyzed for changes in levels of RNAP II (A), total histone H3 (B), acetylated histone 3 (C), histone H3 trimethylated at lysine 27 (D), histone H3 trimethylated at lysine 9 (E), and HP1-α (F). In addition to looking for changes in each of these factors at the promoter-proximal region of the HIV LTR, we also examined the changes in these factors at promoter-proximal regions of the IκBα and GAPDH control genes.

entry into latency has been accumulating from extensive studies demonstrating that there are changes in chromatin structures associated with latent proviruses. As initially noted by Margolis and his colleagues, the presence of histone deacetylases (HDACs) at the HIV LTR is strongly correlated with transcriptional repression leading to latency (18, 30). HDACs are unable to directly associate with proviral DNA but are recruited through cellular DNA-binding proteins that recognize sequences in the viral LTR, including YY1 (18), NF-κB p50 (51), and CBF-1, a CSL [CBF-1, Su(H), and Lag-1]-type transcription factor and key effector of the Notch signaling pathway (45). In addition to the regulation of histone acetylation at the latent provirus, two recent reports demonstrate that the histone methyltransferase Suv39H1, histone H3 methylated on K9, and the repressive HP1 proteins all accumulate on transcriptionally inactive proviruses (9, 36, 37).

In this study, we have confirmed that repressive chromatin markers are present at the LTRs of latent proviruses. In addition to changes in the levels of acetylated H3, we have shown that HP1-α and trimethylated histone H3, with modifications on lysines 9 and 27 (Fig. 8), are present on latent proviruses. In previous studies of histone acetylation during HIV proviral activation, cellular control genes were not examined. To our surprise, our quantitative ChIP assays have demonstrated that compared to the NF-κB-responsive gene IκBα, HIV has very low levels of acetylated histones. Even after proviral activation, the levels of acetylated histones at the HIV LTR are significantly lower than those seen on either the IκBα or GAPDH gene.

Our working hypothesis for the entry of HIV into latency is that blocks to HIV transcription initiation are imposed by these epigenetic silencing mechanisms. This acts to break the Tat-mediated positive regulatory circuit, and once Tat levels fall below threshold levels, the virus is effectively silenced and can become latent. Evidence that breaking the Tat feedback circuit is critical for proviral entry into latency comes from our observation that when Tat is constitutively expressed in *trans*, viral entry into latency is completely blocked (40).

Epigenetic silencing also has been noted in studies of lentiviral vectors carrying internal promoters that have been developed for use in gene therapy (reviewed in reference 11). The shutdown of genes expressed by internal promoters in these vectors appears to be due primarily to repressive elements that are found at the viral promoter. Comparisons between vectors containing either the full-length LTR or self-inactivating vectors carrying deletions in the LTR have established that the shutdown of promoters in *cis* is enhanced by sequences in the U3 region (40).

Attenuation of Tat promotes entry into latency. We have found that the inclusion of the H13L mutation in Tat leads to both a much more rapid shutdown of HIV transcription and a much higher proportion of latently infected cells than that of the wild-type Tat. The H13L mutation is a naturally occurring Tat variant that was first identified in the latently infected U1 cell line (12). Although Reza et al. (42) reported that H13L Tat has a poor ability to *trans*-activate due to reduced interactions between Tat and its cellular cofactor P-TEFb, we have found that lentiviral vectors carrying the H13L Tat in *cis* are able to maintain robust d2EGFP expression at wild-type levels for prolonged periods of time (Fig. 2) and that latent clones carrying the mutation are fully inducible, suggesting that H13L is fully active when it is expressed in sufficient amounts. Nonetheless, it seems likely that the reduced affinity of H13L Tat for P-TEFb makes it inefficient at low concentrations of Tat and thus facilitates the rapid shutdown in transcription that we have observed.

The attenuation of Tat also may play a role in the establishment of latency in vivo. Reza et al. (42) have shown that viruses isolated from patients frequently have defects in Tat that lower its affinity for P-TEFb, including two other naturally occurring Tat sequences, WHC and WHD, which had reduced *trans*-activation activity.

From an experimental perspective, the use of H13L Tat to enhance HIV entry into latency has allowed us to rapidly and reproducibly establish latently infected clones and study their reactivation. The method also facilitates the isolation of latently infected clones of proviruses carrying mutations.

Kinetic analysis of proviral reactivation defines parameters dictating latency. The most precise way to evaluate the behavior of latently infected clones is to study the kinetics of proviral reactivation. Here, we have used ChIP assays to measure the rate of RNAP II recruitment to the promoter and the efficiency of RNAP II elongation. Characteristically, latently infected cells show a low level of RNAP II accumulated at the promoter but virtually no downstream RNAP II (26). The detailed kinetic studies shown in Fig. 7 emphasize that proviral reactivation following NF-κB mobilization by TNF-α results in sequential waves of RNAP II recruitment to the LTR. However, as also noted by Williams et al. (53), because Tat levels are reduced in the latently infected cells, there is a delay of 2 to 4 h before new Tat synthesis results in the efficient elongation of the RNAP II. Kinetic evaluations of latently infected cells that carry proviruses with the C22G mutation in Tat confirm that Tat is strictly required for HIV elongation. Similarly, latently infected cells carrying proviruses with mutations in the NF-κB-binding sites were unable to recruit RNAP II to the promoter.

The reactivation kinetics of clones carrying either the wild-type Tat (clone E4) or H13L Tat (i.e., clones 2D10 and 6) are very similar (data not shown). This is consistent with the idea that all latently infected cells, regardless of the intrinsic activity of their Tat phenotype, are shut down due to similar chromatin-mediated blocks to initiation.

Spontaneous activation and shutdown of latently infected clones. The idea that stochastic fluctuation in Tat levels is a critical event in the switch between the lytic and latent life cycle of HIV has been strongly supported by the computational modeling of Weinberger et al. (47–49). However, their modeling work focused on Tat alone and did not account for the impact of cellular transcription factors, or epigenetic silencing, on the establishment and emergence of HIV from latency.

Here, we report that individual latently infected clonal populations show characteristic frequencies of spontaneously activated cells (Fig. 6). The simplest model to explain its behavior is that depending on the integration sites, there are different degrees of transcriptional silencing that can be imposed and, therefore, different thresholds for activation.

In contrast to these spontaneous events, the activation of latently infected clones by NF-κB induction is remarkably uniform, with all the clones we have examined showing similar patterns of RNAP II distribution on the provirus, rates of

activation, and rates of shutdown. Characteristically, transcriptional shutdown following activation by NF-κB is biphasic (Fig. 5). There is an initial monotonic decline in expression levels due to reductions in initiation as NF-κB levels fall, which is followed by a much slower decline as Tat levels fall. FACS analysis has shown that during this second phase there is a great deal of variation in the transcription of individual cells within the population, which is probably a consequence of both the cell-specific nature of epigenetic silencing events and the stochastic nature of the Tat feedback mechanism.

Cellular models for HIV latency. The rarity of latently infected cells in HIV patients and the lack of a suitable primary cell-based experimental model for HIV latency that permits detailed biochemical analysis and the screening of drugs have necessitated the use of transformed cell lines to model HIV latency. Virtually all molecular studies of HIV latency, including the experiments reported here, have made use of the Jurkat T-cell line as a host cell, since it carries a functional T-cell receptor signaling apparatus that accurately recapitulates many steps in memory T-cell reactivation. Although the relationship between HIV-1 latency occurring in infected patients and in the Jurkat T-cell model is not fully understood, there certainly are many close parallels in the behavior of the latent proviruses in both systems. For example, latent proviruses contained in Jurkat T cells are preferentially integrated into actively transcribed genes, as has been observed for infected resting $CD4^+$ T cells isolated from HIV-infected patients with the effective suppression of viremia (17, 33). In latently infected cells isolated from patients and latently infected Jurkat T cells, the addition of HDAC inhibitors induces latent proviruses, suggesting that chromatin restrictions play a universal role in maintaining latency (54). However, there are clearly important differences between latency in Jurkat T cells and in primary T cells obtained from patients. For example, the transformed Jurkat T cells do not show the restrictions in P-TEFb levels seen in primary lymphocytes. Furthermore, entry into latency in primary cells is likely to be accelerated by differentiation events that are not reproduced in the Jurkat T-cell model.

To address these limitations, there has been an intensive effort by many laboratories to develop a primary cell model for HIV latency. In experiments to be described elsewhere, we have been able to show that primary $CD4^+$ T cells that have been infected by H13L viruses also show a progressive shutdown of HIV transcription that leads to latency. The latent proviruses also have heterochromatic markers on their chromatin (M. Tyagi, R. Pearson, and J. Karn, unpublished observations). Thus, we strongly suspect that the underlying epigenetic mechanisms promoting entry into latency that we have described here also can occur in vivo. Latent HIV proviruses, in any cell type, will show restricted transcription initiation due to the imposition of heterochromatic structures at the viral LTR and restricted transcription elongation because Tat levels have been reduced to sub-threshold amounts.

ACKNOWLEDGMENTS

We thank our colleagues Uri Mbonye, Julian Wong, Julie Jadlowsky, Amzie Pavlisin, Zafeiria Athanasiou, and Michael Lobritz for their help.

This work was supported by NIH grant AI067093 to J.K., the Case CFAR (AI036219), and by grant number 106639-38-RFRL to Y.K.K. from AmfAR, The Foundation for AIDS Research. R.P. was supported by the Geographic Medicine and Infectious Diseases Training Grant (T32-AI07024). K.L. was supported by a postdoctoral fellowship from the Francis Goelet Foundation, the Mathilde Krim fellowship (106999-43-RFRL) from AmfAR, and T32-AI07024.

REFERENCES

1. **Arlen, P. A., D. G. Brooks, L. Y. Gao, D. Vatakis, H. J. Brown, and J. A. Zack.** 2006. Rapid expression of human immunodeficiency virus following activation of latently infected cells. J. Virol. **80:**1599–1603.
2. **Barboric, M., and B. M. Peterlin.** 2005. A New Paradigm in eukaryotic biology: HIV Tat and the control of transcriptional elongation. PLoS Biol. **3:**e76.
3. **Bourgeois, C. F., Y. K. Kim, M. J. Churcher, M. J. West, and J. Karn.** 2002. Spt5 cooperates with Tat by preventing premature RNA release at terminator sequences. Mol. Cell. Biol. **22:**1079–1093.
4. **Brooks, D. G., P. A. Arlen, L. Gao, C. M. Kitchen, and J. A. Zack.** 2003. Identification of T cell-signaling pathways that stimulate latent HIV in primary cells. Proc. Natl. Acad. Sci. USA **100:**12955–12960.
5. **Brooks, D. G., S. G. Kitchen, C. M. Kitchen, D. D. Scripture-Adams, and J. A. Zack.** 2001. Generation of HIV latency during thymopoiesis. Nat. Med. **7:**459–464.
6. **Cannon, P., S.-H. Kim, C. Ulich, and S. Kim.** 1994. Analysis of Tat function in human immunodeficiency virus type 1-infected low-level-expression cell lines U1 and ACH-2. J. Virol. **68:**1993–1997.
7. **Chen, B. K., M. B. Feinberg, and D. Baltimore.** 1997. The κB sites in the human immunodeficiency virus type 1 long terminal repeat enhance virus replication yet are not absolutely required for viral growth. J. Virol. **71:**5495–5504.
8. **Corish, P., and C. Tyler-Smith.** 1999. Attenuation of green fluorescent protein half-life in mammalian cells. Protein Eng. **12:**1035–1040.
9. **du Chéné, I., E. Basyuk, Y. L. Lin, R. Triboulet, A. Knezevich, C. Chable-Bessia, C. Mettling, V. Baillat, J. Reynes, P. Corbeau, E. Bertrand, A. Marcello, S. Emiliani, R. Kiernan, and M. Benkirane.** 2007. Suv39H1 and HP1gamma are responsible for chromatin-mediated HIV-1 transcriptional silencing and post-integration latency. EMBO J. **26:**424–435.
10. **Dull, T., R. Zufferey, M. Kelly, R. J. Mandel, M. Nguyen, D. Trono, and L. Naldini.** 1998. A third-generation lentivirus vector with a conditional packaging system. J. Virol. **72:**8463–8471.
11. **Ellis, J.** 2005. Silencing and variegation of gammaretrovirus and lentivirus vectors. Hum. Gene Ther. **16:**1241–1246.
12. **Emiliani, S., W. Fischle, M. Ott, C. van Lint, C. A. Amella, and E. Verdin.** 1998. Mutations in the Tat gene are responsible for human immunodeficiency virust type 1 postintegration latency in the U1 cell line. J. Virol. **72:**1666–1670.
13. **Fujinaga, K., D. Irwin, Y. Huang, R. Taube, T. Kurosu, and B. M. Peterlin.** 2004. Dynamics of human immunodeficiency virus transcription: P-TEFb phosphorylates RD and dissociates negative effectors from the transactivation response element. Mol. Cell. Biol. **24:**787–795.
14. **Garber, M. E., P. Wei, V. N. KewelRamani, T. P. Mayall, C. H. Herrmann, A. P. Rice, D. R. Littman, and K. A. Jones.** 1998. The interaction between HIV-1 Tat and human cyclin T1 requires zinc and a critical cysteine residue that is not conserved in the murine CycT1 protein. Genes Dev. **12:**3512–3527.
15. **Garriga, J., J. Peng, M. Parreno, D. H. Price, E. E. Henderson, and X. Grana.** 1998. Upregulation of cyclin T1/CDK9 complexes during T cell activation. Oncogene **17:**3093–3102.
16. **Ghose, R., L. Y. Liou, C. H. Herrmann, and A. P. Rice.** 2001. Induction of TAK (cyclin T1/P-TEFb) in purified resting $CD4^+$ T lymphocytes by combination of cytokines. J. Virol. **75:**11336–11343.
17. **Han, Y., K. Lassen, D. Monie, A. R. Sedaghat, S. Shimoji, X. Liu, T. C. Pierson, J. B. Margolick, R. F. Siliciano, and J. D. Siliciano.** 2004. Resting $CD4^+$ T cells from human immunodeficiency virus type 1 (HIV-1)-infected individuals carry integrated HIV-1 genomes within actively transcribed host genes. J. Virol. **78:**6122–6133.
18. **He, G., and D. M. Margolis.** 2002. Counterregulation of chromatin deacetylation and histone deacetylase occupancy at the integrated promoter of human immunodeficiency virus type 1 (HIV-1) by the HIV-1 repressor YY1 and HIV-1 activator Tat. Mol. Cell. Biol. **22:**2965–2973.
19. **Herrmann, C. H., R. G. Carroll, P. Wei, K. A. Jones, and A. P. Rice.** 1998. Tat-associated kinase, TAK, activity is regulated by distinct mechanisms in peripheral blood lymphocytes and promonocytic cell lines. J. Virol. **72:**9881–9888.
20. **Ivanov, D., Y. T. Kwak, J. Guo, and R. B. Gaynor.** 2000. Domains in the SPT5 protein that modulate its transcriptional regulatory properties. Mol. Cell. Biol. **20:**2970–2983.
21. **Jordan, A., D. Bisgrove, and E. Verdin.** 2003. HIV reproducibly establishes a latent infection after acute infection of T cells in vitro. EMBO J. **22:**1868–1877.

22. **Kao, S.-Y., A. F. Calman, P. A. Luciw, and B. M. Peterlin.** 1987. Anti-termination of transcription within the long terminal repeat of HIV-1 by Tat gene product. Nature **330:**489–493.
23. **Karn, J.** 1999. Tackling Tat. J. Mol. Biol. **293:**235–254.
24. **Kent, W. J.** 2002. BLAT—the BLAST-like alignment tool. Genome Res. **12:**656–664.
25. **Kim, Y. K., C. F. Bourgeois, C. Isel, M. J. Churcher, and J. Karn.** 2002. Phosphorylation of the RNA polymerase II carboxyl-terminal domain by CDK9 is directly responsible for human immunodeficiency virus type 1 Tat-activated transcriptional elongation. Mol. Cell. Biol. **22:**4622–4637.
26. **Kim, Y. K., C. F. Bourgeois, R. Pearson, M. Tyagi, M. J. West, J. Wong, S. Y. Wu, C. M. Chiang, and J. Karn.** 2006. Recruitment of TFIIH to the HIV LTR is a rate-limiting step in the emergence of HIV from latency. EMBO J. **25:**3596–3604.
27. **Kinoshita, S., L. Su, M. Amano, L. A. Timmerman, H. Kaneshima, and G. P. Nolan.** 1997. The T cell activation factor NF-ATc positively regulates HIV-1 replication and gene expression in T cells. Immunity **6:**235–244.
28. **Kutsch, O., E. N. Benveniste, G. M. Shaw, and D. N. Levy.** 2002. Direct and quantitative single-cell analysis of human immunodeficiency virus type 1 reactivation from latency. J. Virol. **76:**8776–8786.
29. **Lassen, K., Y. Han, Y. Zhou, J. Siliciano, and R. F. Siliciano.** 2004. The multifactorial nature of HIV-1 latency. Trends Mol. Med. **10:**525–531.
30. **Lehrman, G., I. B. Hogue, S. Palmer, C. Jennings, C. A. Spina, A. Wiegand, A. L. Landay, R. W. Coombs, D. D. Richman, J. W. Mellors, J. M. Coffin, R. J. Bosch, and D. M. Margolis.** 2005. Depletion of latent HIV-1 infection in vivo: a proof-of-concept study. Lancet **366:**549–555.
31. **Lenasi, T., X. Contreras, and B. M. Peterlin.** 2008. Transcriptional interference antagonizes proviral gene expression to promote HIV latency. Cell Host Microbe **4:**123–133.
32. **Leonard, J., C. Parrott, A. J. Buckler-White, W. Turner, E. K. Ross, M. A. Martin, and A. B. Rabson.** 1989. The NF-κB binding sites in human immunodeficiency virus type 1 long terminal repeat are not required for virus infectivity. J. Virol. **63:**4919–4924.
33. **Lewinski, M. K., D. Bisgrove, P. Shinn, H. Chen, C. Hoffmann, S. Hannenhalli, E. Verdin, C. C. Berry, J. R. Ecker, and F. D. Bushman.** 2005. Genome-wide analysis of chromosomal features repressing human immunodeficiency virus transcription. J. Virol. **79:**6610–6619.
34. **Lewinski, M. K., M. Yamashita, M. Emerman, A. Ciuffi, H. Marshall, G. Crawford, F. Collins, P. Shinn, J. Leipzig, S. Hannenhalli, C. C. Berry, J. R. Ecker, and F. D. Bushman.** 2006. Retroviral DNA integration: viral and cellular determinants of target-site selection. PLoS Pathog. **2:**e60.
35. **Li, X. D., B. Moore, and M. W. Cloyd.** 1996. Gradual shutdown of virus production resulting in latency is the norm during the chronic phase of human immunodeficiency virus replication and differential rates and mechanisms of shutdown are determined by viral sequences. Virology **225:**196–212.
36. **Marban, C., S. Suzanne, F. Dequiedt, S. de Walque, L. Redel, C. Van Lint, D. Aunis, and O. Rohr.** 2007. Recruitment of chromatin-modifying enzymes by CTIP2 promotes HIV-1 transcriptional silencing. EMBO J. **26:**412–423.
37. **Mateescu, B., B. Bourachot, C. Rachez, V. Ogryzko, and C. Muchardt.** 2008. Regulation of an inducible promoter by an HP1beta-HP1gamma switch. EMBO Rep. **9:**267–272.
38. **Mitchell, R. S., B. F. Beitzel, A. R. Schroder, P. Shinn, H. Chen, C. C. Berry, J. R. Ecker, and F. D. Bushman.** 2004. Retroviral DNA integration: ASLV, HIV, and MLV show distinct target site preferences. PLoS Biol. **2:**E234.
39. **Nabel, G., and D. A. Baltimore.** 1987. An inducible transcription factor activates expression of human immunodeficiency virus in T cells. Nature **326:**711–713.
40. **Pannell, D., C. S. Osborne, S. Yao, T. Sukonnik, P. Pasceri, A. Karaiskakis, M. Okano, E. Li, H. D. Lipshitz, and J. Ellis.** 2000. Retrovirus vector silencing is de novo methylase independent and marked by a repressive histone code. EMBO J. **19:**5884–5894.
41. **Persaud, D., Y. Zhou, J. M. Siliciano, and R. F. Siliciano.** 2003. Latency in human immunodeficiency virus type 1 infection: no easy answers. J. Virol. **77:**1659–1665.
42. **Reza, S. M., M. Rosetti, M. B. Mathews, and T. Pe'ery.** 2003. Differential activation of Tat variants in mitogen-stimulated cells: implications for HIV-1 postintegration latency. Virology **310:**141–156.
43. **Rice, A. P., and C. H. Herrmann.** 2003. Regulation of TAK/P-TEFb in CD4+ T lymphocytes and macrophages. Curr. HIV Res. **1:**395–404.
44. **Song, S. K., H. Li, and M. W. Cloyd.** 1996. Rates of shutdown of HIV-1 into latency: roles of the LTR and tat/rev/vpu gene region. Virology **225:**377–386.
45. **Tyagi, M., and J. Karn.** 2007. CBF-1 promotes transcriptional silencing during the establishment of HIV-1 latency. EMBO J. **26:**4985–4995.
46. **Wei, P., M. E. Garber, S.-M. Fang, W. H. Fischer, and K. A. Jones.** 1998. A novel cdk9-associated c-type cyclin interacts directly with HIV-1 Tat and mediates its high-affinity, loop specific binding to TAR RNA. Cell **92:**451–462.
47. **Weinberger, L. S., J. C. Burnett, J. E. Toettcher, A. P. Arkin, and D. V. Schaffer.** 2005. Stochastic gene expression in a lentiviral positive-feedback loop: HIV-1 Tat fluctuations drive phenotypic diversity. Cell **122:**169–182.
48. **Weinberger, L. S., R. D. Dar, and M. L. Simpson.** 2008. Transient-mediated fate determination in a transcriptional circuit of HIV. Nat. Genet. **40:**466–470.
49. **Weinberger, L. S., and T. Shenk.** 2007. An HIV feedback resistor: auto-regulatory circuit deactivator and noise buffer. PLoS Biol. **5:**e9.
50. **West, M. J., A. D. Lowe, and J. Karn.** 2001. Activation of HIV transcription in T cells revisited: NF-κB p65 stimulates transcriptional elongation. J. Virol. **75:**8524–8537.
51. **Williams, S. A., L. F. Chen, H. Kwon, C. M. Ruiz-Jarabo, E. Verdin, and W. C. Greene.** 2006. NF-κB p50 promotes HIV latency through HDAC recruitment and repression of transcriptional initiation. EMBO J. **25:**139–149.
52. **Williams, S. A., and W. C. Greene.** 2007. Regulation of HIV-1 latency by T-cell activation. Cytokine **39:**63–74.
53. **Williams, S. A., H. Kwon, L. F. Chen, and W. C. Greene.** 2007. Sustained induction of NF-κB is required for efficient expression of latent human immunodeficiency virus type 1. J. Virol. **81:**6043–6056.
54. **Ylisastigui, L., N. M. Archin, G. Lehrman, R. J. Bosch, and D. M. Margolis.** 2004. Coaxing HIV-1 from resting CD4 T cells: histone deacetylase inhibition allows latent viral expression. AIDS **18:**1101–1108.